American Mineralogist, Volume 89, pages 1822–1825, 2004

LETTER

Coupled cation and oxygen-isotope exchange between alkali feldspar and aqueous chloride solution

THEODORE C. LABOTKA,[1,*] DAVID R. COLE,[2] MOSTAFA FAYEK,[1] LEE R. RICIPUTI,[2] AND FRANK J. STADERMANN[3]

[1]Department of Earth and Planetary Sciences, University of Tennessee, Knoxville, Tennessee 37996-1410, U.S.A.
[2]Chemical Sciences Division, Oak Ridge National Laboratory, Oak Ridge, Tennessee 37831-6110, U.S.A.
[3]Department of Physics, Washington University, St. Louis, Missouri 63130, U.S.A.

ABSTRACT

Nanoscale isotope and chemical images of grains of Amelia albite that were reacted with 2 *m* ^{18}O-enriched solution of KCl show a correspondence between O-isotope exchange and K-Na exchange. Experiments were conducted for 4–6 d at 600 °C and 200 MPa. After 6 d, the 150 μm diameter albite grains had 5–20 μm rims in which Na was nearly completely replaced by K and in which the O was strongly enriched in ^{18}O. The boundary between the core albite and the K-feldspar replacement is sharp and decorated with numerous pores. The distribution of Na and K, determined by electron probe microanalysis, is uniform within the core and rim and has an abrupt discontinuity at the interface. No evidence exists for K-Na interdiffusion at the resolution of electron probe. The NanoSIMS shows that the interface is also sharp in the distribution of ^{18}O and ^{16}O. The NanoSIMS image data and the electron probe data were coregistered; principal components analysis of the merged data set shows that 86% of the total variance in the data result from a single principal component loaded by the replacement of Na by K and ^{18}O. The combined electron probe and NanoSIMS analyses indicate that both cation and isotope exchange occurred during solution and reprecipitation of the feldspar.

INTRODUCTION

Numerous examples exist of the coupling of chemical reactions and diffusion in nature. Some of these include crystal growth–nucleation plus diffusion leading to Liesegang rings, oscillatory zoning in crystals, metamorphic differentiation, concretion growth, orbicular patterns, pseudomorphic replacement reactions, and formation of either hydration or dehydration rims. In general, these phenomena involve either the precipitation of a solid product on the surface of an existing grain, or the formation of a reaction zone that moves into a host crystal. Diffusional transport can occur across the newly formed coating or through the reaction zone.

Plagioclase feldspar in hydrothermally altered volcanic rocks commonly shows evidence for both cation and oxygen isotopic exchange, with preservation of the original grain habit and twinning in the albitic–sericitic rims. For example, Cole et al. (2004) showed that oxygen isotopic patterns in altered plagioclase from the Rico, Colorado, paleohydrothermal system exhibit either step profiles, exponential decay profiles, or flat profiles, indicating varying degrees of equilibration.

Alkali feldspars lend themselves to the experimental study of alteration because the complete Na-K solid solution series can be produced by cation exchange from structurally well-characterized, single-phase materials (e.g., Orville 1963, 1967). O'Neil and Taylor (1967) used this method in their classic study of oxygen isotope fractionation between alkali feldspars and Na-K chloride solutions. On the basis of optical and electron microprobe observations, they concluded that the mechanism of oxygen and cation exchange in their experiments involved fine-scale dissolution and redeposition in a thin film at the interface between the exchanged rim and unexchanged core. They observed that the replacement zone was porous, allowing enhanced communication between the fluid and the reaction interface. Porosity development in altered feldspars is not uncommon and can lead to increased surface area and surface roughness (Hodson 1989). The nature of this microporous zone and communication across it has profound implications on the extent of equilibration of mobile species, including the light elements O, C, and H.

Despite numerous studies detailing the nature of Na-K exchange in anhydrous systems (e.g., Brady and Yund 1983; Christoffersen et al. 1983), a systematic study of the rates of pseudomorphic reaction-front replacement during hydrothermal cation exchange and associated isotopic exchange has not been conducted. We have begun a series of experiments in the alkali feldspar system to determine the correspondence between cation and isotope exchange and the growth of replacement fronts during reaction. In this study we document the exchange in Amelia albite with the aid of the Cameca NanoSIMS, which provides a remarkable compositional image of the reaction interface at the nanoscale.

METHODS

Hydrothermal experiments

Crystals of Amelia albite were crushed into powders that were repeatedly washed in deionized water and sieved to remove any ultra-fine particles (<1–2

* E-mail: tlabotka@utk.edu

μm). For this study, we selected grains ranging in diameter from about 50 to 200 μm. Albite was reacted with ^{18}O-enriched KCl (aq) (1 and 2 m) at 600 °C and 200 MPa for 4, 5, and 6 days. Samples were sealed in Au capsules, which were loaded into standard horizontally mounted hydrothermal cold-seal vessels. A typical charge consisted of ~15 mg of feldspar powder and ~30 mg of aqueous chloride solution made from anhydrous KCl and 98+ at% ^{18}O water (Cambridge Isotope Laboratories, OLM-240). For these experiments we used only one temperature and pressure: 600 °C and 200 MPa. The total run-up time to temperature (controlled to ±1 °C) was approximately 20 min., and runs were quenched isobarically in an air stream aided by cold water to below 100 °C in ~10 min. Capsules were rejected if the weight of the capsule after the experiment differed by more than ~0.1% from the original weight of 1.0–1.5 g. Powders retrieved from each capsule were repeatedly rinsed in deionized water to remove any salt. Two splits of each sample were prepared, one for subsequent assessment by scanning electron microscopy (SEM), and a second for standard thin section mounts suitable for both electron probe microanalysis (EPMA) and secondary ion mass spectrometry (SIMS).

Analytical techniques

After experimentation, the powders were examined by several techniques, which included standard optical microscopy, SEM, EPMA, and SIMS (or ion microprobe). SEM observations showed no evidence of crushing of grains nor any sign of fine-grained quench products. EPMA was used to determine the Na/K ratios quantitatively in the reaction rims and to generate X-ray maps of Na and K in select grains. Quantitative analyses of Si, Al, Fe, Ca, Na, and K were conducted with a Cameca SX50 electron microprobe at the University of Tennessee, Knoxville, with a beam current of 30 nA, wavelength dispersive spectrometers, and natural mineral standards. Relative errors are typically <± 3% for major elements. The measured composition of the Amelia albite starting material is $Ab_{97}Or_2An_1$. X-ray images were collected by the same wavelength-dispersive spectrometers with counting times of ~150 ms. Back-scattered electron (BSE) images were obtained at the same time.

High-resolution (~50 nm) SIMS images were obtained with a CAMECA NanoSIMS 50, at Washington University, St. Louis. A focused 50 nm Cs+ primary ion beam accelerated at 16 kV was used to raster over the sample surface, and negative secondary ions were extracted with –8 kV. Both isotopes of oxygen (^{16}O- and ^{18}O-) were detected simultaneously with the multi-collector, electron multiplier ion-counting system. Typical analyses lasted approximately 5 minutes.

RESULTS

Distribution of K and Na

The albite starting materials were optically clear, whereas albite run products showed obvious reaction with the chloride solutions; the reacted samples are cloudy from numerous pores. In thin section, the pores are concentrated at the boundary between the unreacted core and the replacement rim. We didn't observe any pores or channels extending from the boundary to the surface of the grains. The rims increase in width from 5–10 μm in the four-day experiment to 20–30 μm in the six-day experiment. We were unable to tell whether the rims are in optical continuity with the host, although this is commonly observed in other studies of mineral replacement (Putnis 2003).

Overgrowths are readily observed in both BSE and X-ray images of thin sections. The replacement rims are in sharp contact with the core grains, and the thickness of the rims is generally greater on grains from the longer-duration experiments, although the thickness varies because of the orientation effects produced by thin sectioning. Figure 1 is a composite image of one grain of Amelia albite, reacted with 2 m KCl for 6 d. The image is 24-bits deep and combines X-ray images for Na$K\alpha$ in the red channel and K$K\alpha$ in the green and blue channels. The dark-red regions in the core are Na-rich, and the cyan-colored rim is K-rich. The boundary between the host albite and the potassic rim is decorated with numerous pores of various sizes.

Quantitative analyses across the interface are shown in Figure 2. The rim compositions are those of a K-feldspar with a formula near $K_{0.85}Na_{0.15}AlSiO_8$. There is no detectable Fe, and Ca is at or below the detection limit. Analyses of the 6 d experiment, shown in Figure 2, are spaced 2 μm and show small, unsystematic variation in K/(K + Na) in the rim. At the 2 μm scale, the boundary between rim and core is abrupt. The 5 d experiment seems to have a wider rim, but that appears to be an artifact of the slice through the grain because the rims are much narrower in other grains in the same section. There appears to be an increase in K/(K + Na) in the potassic rim near the interface, but the increase is not seen in the longer experiment and could be a result of analytical uncertainty. The K/(K + Na) ratio of the host and replacement rim at the interface appear to be 0.05 (the starting composition) and 0.85, respectively. The equilibrium compositions determined by Orville (1963) for 200 MPa and 600 °C are Or_{10} and Or_{63}, but we did not see those compositions at the ~2 μm scale. The analyzed rims in all experiments have K/(K + Na) ≥0.85, and the cores all retain the original albite composition.

Distribution of ^{18}O and ^{16}O

A grain of Amelia albite from the six-day experiment was imaged with the NanoSIMS and is shown in Figure 3. The ^{18}O-rich region, shown on the left side of Figure 3A, is in sharp contact with the ^{16}O-rich region, even at the 50–100 nm scale of the NanoSIMS image. The X-ray micrograph of the same region, shown in Figure 3B, shows the same features as the ion image, even though the spatial resolution of the X-ray image is much poorer. For example, a small embayment near a pore on the left side of both images can be seen in both the NanoSIMS (Fig. 3A) and the X-ray (Fig. 3B) images. The ^{18}O-exchanged area seems to correspond precisely with K-exchanged area, even in the fine detail shown in Figure 3.

The correspondence between the ion and X-ray images was tested with principal components analysis. The data sets were first coregistered using standard image-processing techniques, with the use of the program ENVI (Research Systems, Inc.). The result is a 256 × 256 data set having four eight-bit bands covering the area common to both images. Eigenvectors were determined for the covariance matrix; their direction cosines are given in Table 1. The first eigenvector accounts for 86% of the total variance. This vector is equally weighted in ^{18}O and K and is negatively weighted in Na.

The relation is better seen in the correlation coefficients, given in Table 1. K and ^{18}O are strongly correlated, and they are inversely correlated with Na. There is little correlation with ^{16}O because even in the ^{18}O-enriched zones, 65% (uncorrected) of the O is ^{16}O. The second principal component, accounting for 7% of the variance, is essentially ^{16}O, which is probably a result of the uncorrected $^{18}O/(^{18}O + ^{16}O)$ ratio for the NanoSIMS data. If the true O-isotope ratio in the exchanged rim is closer to 1.0, then all the variance would be in the first principal component.

Even though the boundary between the exchanged and unexchanged regions is sharp, evidence exists suggesting that diffusion occurred in the host albite. The ion image in Figure 4 is an enlargement of the left-center of the grain in Figure 3A. The image is contoured in the $^{18}O/(^{18}O + ^{16}O)$ percentage with a line profile shown on the right. The ratios are uncorrected for

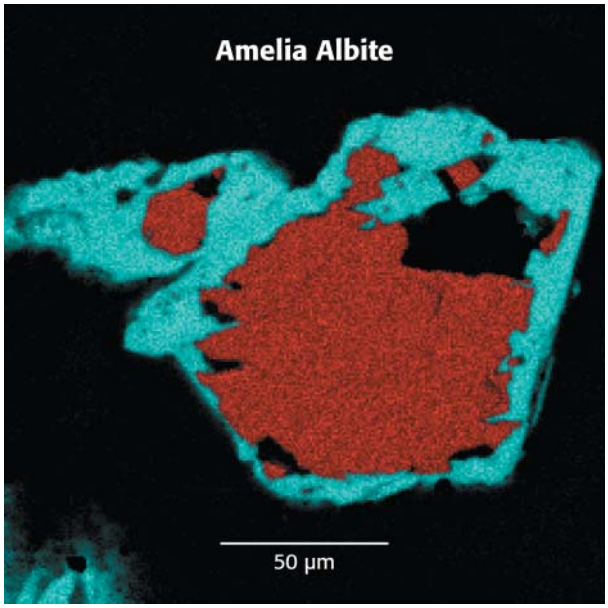

FIGURE 1. Amelia albite reacted with 2 *m* KCl solution for 6 d, at 600 °C, 200 MPa. The image is a composite of Na*K*α in the red channel and K*K*α in the blue and green channels. The dark core of the grain is the starting albite, and the light rim is K-feldspar. Note the pores at the interface.

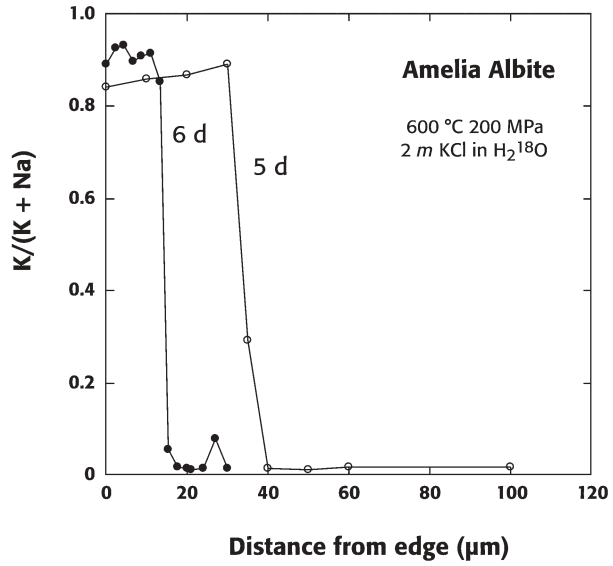

FIGURE 2. Quantitative analyses across the reaction interface in the grain shown in Figure 1 (6 d) and in another grain from a 5 d experiment. The boundary between albite and K-feldspar is sharp at the 2 µm scale of the electron probe microanalyses.

instrumental mass-bias effects associated with NanoSIMS images and are only semiquantitative. The NanoSIMS indicates a maximum ratio of 0.38, but the actual value may be much higher. Analyses of the rims of other grains indicate fractions as high as 0.9. In the profile shown in Figure 4B, the $^{18}O/(^{18}O + ^{16}O)$ ratio drops from a value of ~0.35 to 0.0 within 670 nm, which is five to ten times the spatial resolution of the NanoSIMS.

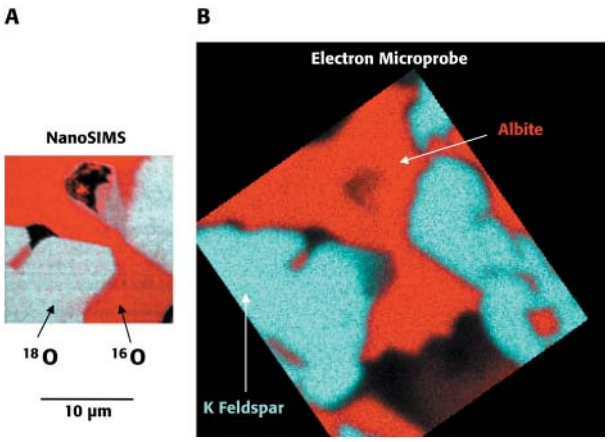

FIGURE 3. NanoSIMS and X-ray images of a grain of Amelia albite from a 6 d experiment. (A) NanoSIMS image of an ^{18}O-enriched rim on the host albite core. ^{18}O is in the blue and green channels and ^{16}O is in the red channel of the ion image. (B) Na is in the red channel, and K is in the blue and green channels of the X-ray image. The X-ray image is coregistered with the ion image to create a combined data set for the common area.

TABLE 1. Principal components and correlation coefficients for the merged X-ray and ion image data

	Principal components			
	PC 1	PC 2	PC 3	PC 4
^{18}O	0.570	0.260	–0.758	0.182
^{16}O	–0.054	0.920	0.194	–0.337
K	0.590	0.100	0.604	0.526
Na	–0.570	0.277	–0.151	0.759
% Variance	86	7	4	3

	Correlation Coefficients			
	^{18}O	^{16}O	K	Na
^{18}O	1.00			
^{16}O	–0.11	1.00		
K	0.86	–0.13	1.00	
Na	–0.87	0.27	–0.91	1.00

DISCUSSION

The high correlation between cation and isotope distribution indicates that the exchange resulted from the same process. Not only are the alkali atoms replaced, but so are the O atoms, which indicates the wholesale reconstruction of the feldspar. The cation exchange was driven by the large difference in the free energy between the nearly pure-Na feldspar and the KCl solution. The result is the precipitation of a feldspar with a composition in apparent equilibrium with the fluid. That the exchange occurred by solution–precipitation rather than by diffusion is indicated by the coincident replacement of the O by the ^{18}O from the fluid, the constancy of the ratios $^{18}O/(^{18}O + ^{16}O)$ and K/(K + Na), and the numerous pores at the interface between the overgrowth and the core grain. Similar relations were observed by Schliestedt and Matthews (1987) in experiments with intermediate plagioclase and $CaCl_2$ solution.

The diffusivity of O in albite is approximately 5×10^{-15} cm^2/s at 600 °C, 200 MPa (Giletti et al. 1978; Yund et al. 1981; Cole and Chakraborty 2001). The O-diffusion depth expected in albite after six days is approximately 0.5 µm, similar to the width of the zone shown in Figure 4B. The apparent diffusion

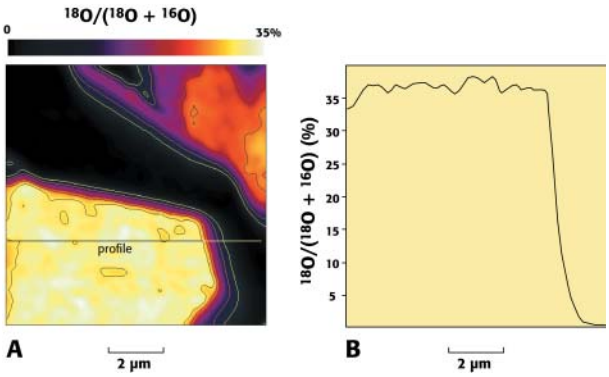

FIGURE 4. (A) Contours of $^{18}O/(^{18}O + ^{16}O)$, expressed as percent, in an enlarged portion of Figure 3A. (B) Profile along the line shown in A. The ratio is uncorrected and is semiquantitative. The drop in the ratio occurs over a distance that is 5–10 times the spatial resolution of the NanoSIMS.

profile in Figure 4B can be fitted to the simple relation erfc(x/2) with a diffusion coefficient of 2.9×10^{-15} cm^2/s. That value, however, depends on the unknown mass bias correction for the NanoSIMS. If the discrimination is linear, then the derived value of D depends only on the slope of the profile, and D remains 2.9×10^{-15} cm^2/s. That value doesn't account for the movement of the interface as exchange continues and so is only an estimate. It is notably similar, though, to values determined by others (Cole and Chakraborty 2001). The diffusivity also depends on crystallographic direction, as can be discerned from the contours shown in Figure 4A. Diffusion may indeed have occurred at the interface, but it was clearly subordinate to solution and growth of the new feldspar rim.

Evidence for diffusion of Na and K across the interface was not detected in our analyses of the experimental products. Tracer diffusion coefficients for K and Na in orthoclase were measured by Foland (1974) and found to be $\sim 3 \times 10^{-16}$ cm^2/s and $\sim 3 \times 10^{-13}$ cm^2/s, respectively, at 600 °C and 200 MPa. The K-Na interdiffusion in alkali feldspar was measured by Brady and Yund (1983) at 600 °C and was found to be $2–4 \times 10^{-17}$ cm^2/s for intermediate composition feldspar. The value of D predicted by a Darken model for interdiffusion in albite (Brady and Yund 1983; Christoffersen et al. 1983) is $\sim 10^{-15}$ cm^2/s. The range of values implies a diffusion distance of ~ 225–125 nm in the albite in the six-day experiment. All those experiments were conducted without H_2O, however. The presence of H_2O commonly accelerates diffusion (Cole and Chakraborty 2001), and the diffusion distance in our experiments may be greater. Although diffusion of Na and K may have occurred across the interface, it occurred on a scale too small to be discerned by the electron microprobe, ≤2 μm.

The K-feldspar rims on Amelia albite are the result of dissolution and reprecipitation. This process was certainly driven by the large affinity between albite and the KCl solution. Although not presented here, our experiments with sanidine in NaCl solutions show similar results: an ^{18}O-exchanged rim of Na-feldspar formed on the sanidine core. The exchange is a result of a metasomatic reaction with a fluid out of equilibrium with the original feldspar. The extension to natural replacement reactions, such as that described by Cole et al. (2004), indicates that the correlation between cation and isotope exchange is a result of solution–reprecipitation. NanoSIMS imaging reveals a fine structure on the nanometer scale at the reaction interface showing O exchange between the host albite and its surroundings that is otherwise unobservable with other imaging techniques.

ACKNOWLEDGMENTS

This study was partially support by NSF grants EAR-0106990 and EAR-0087553. D. Cole, M. Fayek, and L. Riciputi gratefully acknowledge the support from the Division of Chemical Sciences, Geosciences, and Biosciences, Office of Basic Energy Sciences, U.S. Department of Energy, under contract DE-AC05-00OR22725, Oak Ridge National Laboratory, managed and operated by UT–Battelle, LLC. We sincerely appreciate the comments of Associate Editor Andreas Luttge and an anonymous reviewer, which helped to improve the manuscript.

REFERENCES CITED

Brady, J.B. and Yund, R.A. (1983) Interdiffusion of K and Na in alkali feldspar: homogenization experiments. American Mineralogist, 68, 106–111.

Christoffersen, R., Yund, R.A., and Tullis, J. (1983) Inter-diffusion of K and Na in alkali feldspars: diffusion couple experiments. American Mineralogist, 68, 1126–1133.

Cole, D.R. and Chakraborty, S. (2001) Rates and mechanisms of isotopic exchange. In J.W. Valley and D. Cole, Eds., Stable Isotope Geochemistry, 43, 82–223. Reviews in Mineralogy, Mineralogical Society of America, Washington, D.C.

Cole, D.R., Larson, P.B., Riciputi, L.R., and Mora, C.I. (2004) Oxygen isotope zoning profiles in hydrothermally altered feldspars: Estimating the duration of water–rock interaction. Geology, 32, 29–32.

Foland, K.A. (1974) Alkali diffusion in orthoclase. In Hofmann, A.W., Giletti, B.J., Yoder, Jr., H.S., and Yund, R.A., Ed., Geochemical Transport and Kinetics, Publication 634, p. 77–98. Carnegie Institution of Washington, D.C.

Hodson, M.E. (1999) Micropore surface area variation with grain size in unweathered alkali feldspars: Implications for surface roughness and dissolution studies. Geochimica et Cosmochimica Acta, 62, 3429–3435.

Kerrick, D.M., Lasaga, A.C., and Raeburn, S.P. (1991) Kinetics of heterogeneous reactions. In Derrill M. Kerrick, Ed., Contact Metamorphism, 26, 583–671. Reviews in Mineralogy, Mineralogical Society of America, Washington, D.C.

O'Neil, J.R. and Taylor, H.P. (1967) The oxygen isotope and cation exchange chemistry of feldspars. American Mineralogist, 52, 1414–1437.

Orville, P.M. (1963) Alkali ion exchange between vapor and feldspar phases. American Journal of Science, 261, 201–237.

———(1967) Unit-cell parameters of the microcline–low albite and sanidine–high albite solid solution series. American Mineralogist, 52, 55–86.

Putnis, A. (2003) Mineral replacement reactions: From macroscopic observations to microscopic mechanisms. Mineralogical Magazine, 66, 689–708.

Schliestedt, M. and Matthews, A. (1987) Cation and oxygen isotope exchange between plagioclase and aqueous chloride solution. Neues Jahrbuch für Mineralogie Montshefte, 6, 241–248.

MANUSCRIPT RECEIVED APRIL 19, 2004
MANUSCRIPT ACCEPTED SEPTEMBER 29, 2004
MANUSCRIPT HANDLED BY ANDREAS LUTTGE